S. ZHANG©[1,2], Q. HOU©[1], H.Y. JIANG©[1,2*]

A MODIFIED KERNER MODEL TO PREDICT THE THERMAL EXPANSION COEFFICIENT OF MULTI-PHASE REINFORCED COMPOSITES Al6092/SiC/LAS

In this work, a new supplementary formula was introduced to modify the Kerner model. This supplementary formula enable the Kerner model to predict the thermal expansion coefficient of multi-phase reinforced composites by normalization of the thermal expansion coefficient, bulk modulus, and shear modulus of the reinforcements. For comparison, the modified Kerner model as well as modified Schapery, the rule of mixtures, and Turner models were used to predict the thermal expansion coefficient of multi-phase reinforced composites 6092 Aluminum Alloy/silicon carbide/β-eucryptite. The results confirm the robustness of the modified Kerner model for predicting the thermal expansion coefficient of composites with multi-phase near-spherical inclusions. It may provide a fine selection to predict the thermal expansion coefficient of multi-phase reinforced metal matrix composites which cannot predict efficiently before.

Keywords: Thermal expansion coefficient; Multi-phase; Normalization; Thermoelastic

1. Introduction

Discontinuous reinforced metal-matrix composites (MMCs) are advanced materials that have attracted considerable interest because of their high-performance isotropic mechanical properties [1]. Aluminum matrix composites (AMCs) are MMCs that are widely used in lining materials, heat sinks, and precision parts in electronic equipment. In these applications, AMCs require high toughness to ensure high mechanical strength, good thermal conductivity to accelerate heat dissipation, and a low coefficient of thermal expansion (CTE) to achieve dimensional stability. Among these factors, optimizing the CTE has attracted extensive attention and research because it is crucial for achieving good service performance. And the CTE of AMCs is influenced by a combination of factors. For example, Zare et al. [2] prepared an Al6061/silicon carbide composite. The results showed that the CTE of the composite decreased significantly with the increase of silicon carbide (SiC) volume fraction. In addition, the CTE increased with increasing temperature. However, this increase shows a nonlinear trend. Esmati et al. [3] considered the effect of anisotropy of the reinforcing phase on the CTE of Al-Graphite composites. Since the CTE of graphene in the *a*-axis and *c*-axis directions is –0.5 and 28 K^{-1}, respectively. This property leads to a large variation in the CTE of the composite in different directions. Tayebi et al. [4] investigated the thermal deformation behavior of Al-B$_4$C composite samples during cooling. The results showed that the CTE changes of the samples showed strain hysteresis during the heating-cooling process of the samples. This was reported to be due to the deformation caused by strain within the structure, which resulted in permanent expansion.

The key to influence the CTE of AMCs is the inherent properties of the each constituents, such as their geometry, distribution, volume fraction, and interfacial bonding characteristics. Expansion strain is generated as an object is subjected to temperature change. The rigidity of reinforcements in composites can constrain this matrix expansion strain, and the strain magnitude depends on the shear transfer at the interface [5]. Therefore, the strain induced by thermal stress strongly depends on elastic constants. Many thermoelastic models are available to predict the elastic constants of composites for the characterization of CTE. Four widely used models have been reported to effectively predict composite CTE values, including the rule of mixtures (ROM) model based on the linear rule for mixtures and the Turner [6], Kerner [7], and Schapery [8] models based on the thermoelastic energy principle. The thermoelastic

1 HUNAN UNIVERSITY OF TECHNOLOGY, SCHOOL OF PACKAGING AND MATERIALS ENGINEERING, ZHUZHOU 412007, CHINA
2 HUNAN UNIVERSITY OF TECHNOLOGY, NATIONAL & LOCAL JOINT ENGINEERING RESEARCH CENTER FOR ADVANCED PACKAGING MATERIAL AND TECHNOLOGY, ZHUZHOU 412007, CHINA

* Corresponding author: jhyun@163.com

models assume that the matrix and reinforcing phases are linearly elastic over a small range of bulk strains and considered homogeneous [9]. It is notable that CTE calculations for multi-phase reinforced composites using thermoelastic models have rarely been reported. This is mainly because most models cannot calculate the CTE of multi-phase reinforced composites due to the condition limitations.

In fact, the ROM and Turner models can predict the CTE of multi-phase reinforced composites. However, the prediction is not satisfying because both models ignore the influence of the angle and distribution of reinforcements and shear deformation for calculating CTE. Moreover, the Turner model assumes that the interface between the particles and the matrix leads to close contact and assumes that expansion occurs at the same speed under uniform hydrostatic pressure [10]. In contrast, the original Kerner and Schapery models are considered more accurate than ROM and Turner models for assuming that reinforcements are discontinuous, spherical, and wetted by a uniform base layer. Therefore, the CTE of a composite is considered identical to that of a volume element composed of a spherical reinforcement particle surrounded by a shell of a matrix. In addition, normal and shear stresses were considered since the shear and bulk modulus were introduced [7]. Because of these, the Kerner and Schapery models have been proved to be robust for predicting the CTE of single-phase reinforced composites CTE [10-13]. But they are only suitable for the CTE calculation of two-phase composites for regarding reinforcements as a kind of particles [14,15]. To overcome this limitation, Tayebi [16] proposed a flexible method to use the two-phase model to predict the CTE of three-phase composites Al/Cu/SiC. The CTE of these composites was calculated using SiC as the reinforcing phase for Cu and SiC/Cu as the reinforcing phase for the Al matrix. Their obtained CTE values calculated with the Turner and Kerner models showed a slight difference (less than 8%). However, this approach is limited because the reinforcing phases need to form an enfolding structure. Otherwise, the CTE of reinforcing phases cannot be calculated using a two-phase model. Therefore, the CTE of multi-phase, especially more than three-phase, reinforced composites cannot be obtained easily by using this flexible method.

In this work, a new supplementary formula was introduced to modify the Kerner and Schapery thermoelastic models for calculating the CTE of AMCs with SiC and β-eucryptite (LAS) as reinforcements. As a negative thermal expansion material, LAS can inhibit the outward expansion behavior of the Al matrix when subjected to heat. Therefore, LAS can significantly reduce the CTE of the composites [17]. The experimental and calculated CTE values were compared, and the correlation between the thermoelastic models and the structure and parameters of the composites was analyzed, too. The adaptability of different CTE prediction models to multi-phase reinforced AMCs is also discussed herein. This work provides a basis for predicting and analyzing the thermal expansion behavior of multi-phase reinforced MMCs.

2. Method and materials

2.1. Composites preparation and characteristics

The Al6092/SiC/LAS composites used in this investigation were fabricated using the powder forging method. The composite consisted of 60% Al6092 alloy and 40 wt% SiC, or 35 wt% SiC/5 wt% LAS, or 30 wt% SiC/10 wt% LAS, or 25 wt% SiC/15 wt% LAS, or 20 wt% SiC/20 wt% LAS. A commercial Al6092 ingot was purchased (JIENUO JINSHU, Shanghai). It is powdered at an average particle size of about 48-80 μm by self-developed spray deposition equipment [18]. The main element of Al6092 is Al, with 1.2% Si and 0.8% Mg (mass fraction) also present, as shown in TABLE 1. LAS and SiC were purchased with respective particle sizes of about 1-4 μm and 5-10 μm, respectively. To eliminate moisture, the LAS and SiC particles were pretreated by drying at 100°C for 24 h. A double cone mixer was used to grind the mixtures for 24 h to improve their dispersion and homogeneity. The forging environment was a relative vacuum low than –0.08 MPa. The samples were first preheated and held at 200°C and 400°C for 2 h each, then at 590°C for 1 h. The samples were then forged at a pressure of 14 MPa for 1 min. The forging was repeated twice to obtain ingots.

TABLE 1

Chemical composition of Al6092 alloy

Element	Mass fraction (wt%)
Aluminum, Al	95.35-98.05
Magnesium, Mg	0.80-1.20
Copper, Cu	0.70-1.00
Silicon, Si	0.70-1.30
Iron, Fe	≤0.30
Zinc, Zn	≤0.25
Titanium, Ti	≤0.15
Chromium, Cr	≤0.15
Manganese, Mn	≤0.15
Oxygen, O	0.05-0.50
Other, each	≤0.05
Other, total	≤0.15
Total	100

The microscopic morphology of the composites was characterized by scanning electron microscopy (SEM, AztecFeature, Oxford Instruments). Transmission electron microscopy (TEM, JEM-2100, JEOL Ltd.) was used to reveal the interface morphology. Using a thermal dilatometer (DIL 402C, NETZSCH), the CTE values of the samples were measured from room temperature (RT) to 500°C at a heating rate of 10°C/min in an argon atmosphere. Subsequently, the CTE values of the samples cooled from 500°C to RT were also tested at a cooling rate of 10°C/min. The samples had a diameter of 8 mm and a height of 10 mm. Five samples of the same mass fraction were tested, and their arithmetic mean value was used as the final CTE to eliminate the effect of errors on the uncertainty of the experimental results. The relevant calculation parameters for Al, SiC, and LAS were

obtained from the literature and JMatPro software, and the specific parameters are provided in TABLE 2 [19,20].

Physical properties of Al, SiC, and LAS

	Temperature (°C)	Density (g/cm³)	E (GPa)	G (GPa)	K (GPa)	CTE (×10⁻⁶ K⁻¹)
Al	50	2.70	68.93	25.8	69.93	21.8
	100	2.69	67.18	25.11	69.01	22.4
	150	2.68	65.31	24.37	68.04	23.2
	200	2.67	63.32	23.58	67.01	23.9
	300	2.65	58.88	21.83	64.79	25.9
	400	2.63	53.78	19.84	61.92	27.8
	500	2.60	48.13	17.66	58.36	29.5
SiC	\	3.22	410	192	158	6.58
LAS	\	2.67	83	49	21.18	-6.2

2.2. The Modified Kerner and Schapery models

TABLE 3 shows the thermoelastic models for predicting the CTE of composites. Where Eqs. (1)-(4) are the ROM, Turner, Kerner and Schapery models, respectively. In this work, a normalized process using a new supplementary formula was proposed for reinforcing phases like Eqs. (5)-(7). Then the CTE, bulk modulus, and shear modulus of different reinforcing phases were integrated into new "single" CTE, bulk modulus, and shear modulus according to their respective volume fractions based on the linear rule of mixtures. In these models, the multiple reinforcements are considered uniformly dispersed in composite, ignoring the interaction between reinforcements just like Fig. 1. Additionally, none of the previously reported models for calculating the CTE values of composites incorporate a dependence on particle size, which is necessary to normalization of different particles.

TABLE 3

Thermoelastic models for predict the CTE of composites

Model	Equation	
ROM	$\alpha_c = V_m \alpha_m + \sum_i^n V_i \alpha_i$	(1)
Turner	$\alpha_c = \dfrac{\alpha_m V_m K_m + \sum_i^n \alpha_i V_i K_i}{V_m K_m + \sum_i^n V_i K_i}$	(2)
Kerner	$\alpha_c = \alpha_m V_m + \alpha_p V_p + V_m(1-V_m)(\alpha_p - \alpha_m) \times$ $\times \dfrac{K_p - K_m}{V_m K_m + V_p K_p + \dfrac{3K_m K_p}{4G_m}}$	(3)
Schapery	$\alpha_c = \alpha_p + (\alpha_m - \alpha_p) \times \dfrac{K_m(K_p - K_{H-S})}{K_{H-S}(K_p - K_m)}$	(4)

where: α: CTE; V: volume fraction; K: bulk modulus; G: shear modulus; subscript c: composite; subscript m: matrix; subscripts i and p: reinforcements; superscript l: lower bound; superscript u: upper bound.

$$\alpha_p = \sum_n^i \alpha_p^i \times \frac{V_p^i}{V_{tol}} \tag{5}$$

$$K_p = \sum_n^i K_p^i \times \frac{V_p^i}{V_{tol}} \tag{6}$$

$$G_p = \sum_n^i G_p^i \times \frac{V_p^i}{V_{tol}} \tag{7}$$

Where: the superscript i represents the different reinforcing phases, and the V_{tol} is the total volume of reinforcing phases.
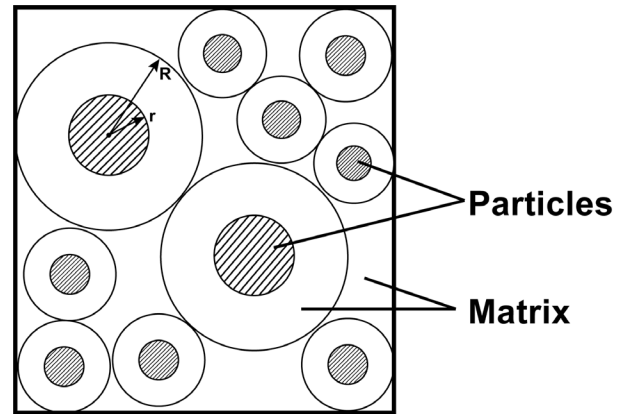

Fig. 1. Uniform dispersion structure of multi-reinforcement in the composites

According to this approach, the α_p, K_p, G_p obtained from Eqs. (5)-(7) can be substituted into the Kerner model. And the Kerner model can be modified as:

$$\alpha_c = \alpha_m V_m + \sum_n^i \alpha_i V_i + V_m(1-V_m)(\alpha_p - \alpha_m) \times$$
$$\times \frac{K_p - K_m}{V_m K_m + \sum_n^i V_i K_p + \dfrac{3K_m K_p}{4G_m}} \tag{8}$$

The Schapery model gives upper and lower bounds for the CTE values using thermoelastic principles, which are provided by the lower (Eq. 9) and upper (Eq. 10) bounds of Hashin-Shtrikman (H-S) Model, respectively [1,21]. The H-S model is based on the macroscopical isotropy and the quasi-homogeneity of the composite, where the shape of the reinforcement is not a limiting factor. According to this approach, both the upper and lower bounds of modified Schapery model can be used to calculate the CTE of multi-phase reinforced composites.

$$K_l = K_m + \frac{V_p}{\dfrac{1}{K_p - K_m} + \dfrac{V_m}{K_m + \dfrac{4}{3}G_m}} \tag{9}$$

$$K_u = K_p + \frac{V_m}{\dfrac{1}{K_m - K_p} + \dfrac{1-V_m}{K_p + \dfrac{4}{3}G_p}} \tag{10}$$

1330

3. Results and discussion

The CTE variation of the samples with temperature is shown in Fig. 2, which is obtained from the experimental values and the predicted values using thermoelastic models at a different compounding rate. For the low-temperature interval, the experimental CTE values show a rapid increase between room temperature (RT) and 200°C, which is not consistent with any of the thermoelastic models. This deviation between the predicted and experimental values is potentially related to the thermal mismatch stresses caused by the significant CTE difference between the matrix and reinforcing phases [16,22]. In the high-temperature interval (>200°C), it is evident that the predicted values calculated by the Kerner model show a good coincidence with all the experimental CTE values. For example, in the sample containing 25 wt% SiC/15 wt% LAS, the difference of CTE is only 0.74% at 500°C. This indicates the effectiveness of the normalization process for predicting the CTE of multi-phase particle-reinforced composites. For the Schapery model, all the experimental CTE almost approach the upper bound values. In fact, the upper bound values of the Schapery model coincide with the predicted values of the Kerner model. Because the Hashin's lower bound for bulk modulus is stated to be an exact result for predicting elastic composites regarding the reinforcement as a sphere coated with a uniform matrix layer [9]. This is consistent with the idealized assumptions of the Kerner model for the structure of particle-reinforced composites. It should be noted that the zoom calculated using the Schapery model covered most experimental CTE values, the region is often too large and

sometimes impractical. It cannot provide a relatively acceptable numerical solution like the Kerner model.

Fig. 3 shows a comparison of the predicted and experimental CTE values of the composites with different reinforcement mass fractions at 500°C. Its clearly shows the trend of CTE values for different reinforcement mass fractions and the superiority of Kerner model in predicting CTE of multiphase particle-reinforced AMCs is highlighted. It is worth noting that increasing LAS content is accompanied by a decrease in the composite CTE except for the Turner model, which has an apparent downward linear trend because LAS has a lower CTE than SiC. In contrast, the CTE results calculated by the Turner model show an anomalous upward trend with increasing LAS mass fraction. Obviously, this result does not correlate with real-world conditions. This is because the Turner model overly relies on bulk modulus, which requires the components to have the same bulk modulus or the same modulus in terms of composition and weight ratio. However, the bulk modulus values of SiC and LAS are too dissimilar compared to the bulk modulus of the Al matrix, which indicate that the phases differ in their ability to resist deformation when heated. Therefore, the composites inevitably generate internal stress during the thermal expansion process, resulting in an error between the Turner model calculation value and the experimental result. In addition, SiC has a high bulk modulus and a low CTE compared to the Al matrix. while concerning on LAS particles, both the CTE and bulk modulus values are lower than those of the Al matrix, which is the opposite of most of the metal matrix composites studied so far. This is also a paradoxical upward deviation of the CTE
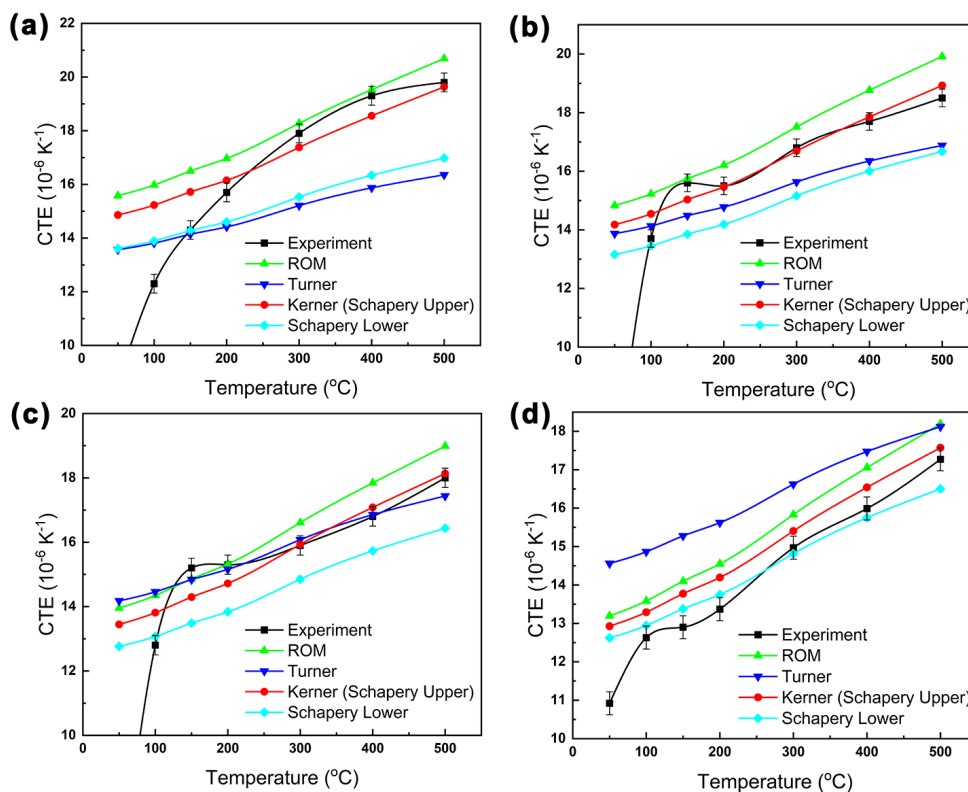

Fig. 2. The experimental and model predicted CTE values of composites: (a) 35 wt% SiC/5 wt% LAS, (b) 30 wt% SiC/10 wt% LAS, (c) 25 wt% SiC/15 wt% LAS, and (d) 20 wt% SiC/20 wt% LAS
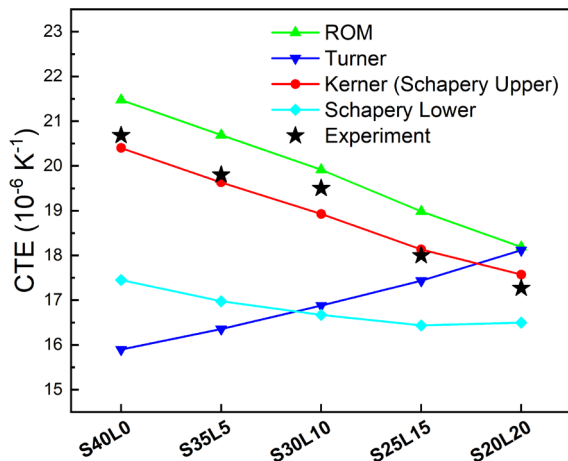
Fig. 3. Comparison of predicted and experimental CTE values at 500°C (S refers to SiC and L refers to LAS)

effect of LAS. In the experimental group, the bulk modulus of the reinforcing phase in the 20 wt% SiC/20 wt% LAS composite remained 89.59 Gpa, which is higher than that of the Al matrix (69.93 Gpa). As a result, it can be seen in Fig. 4 that the Kerner model maintains an overall decreasing trend.

Furtherly, SEM and TEM were performed to charcaterize the composite structure (Fig. 4). As shown in Fig. 4a, SiC and LAS are uniformly dispersed in the Al matrix permeated and packed by the Al matrix. Fig. 4b and 4c show the interfacial characteristics of SiC and LAS with Al matrix, respectively. Based on our previous work, it can be shown that SiC and LAS exhibit tight interfacial connections with Al grains, which present an interfacial bonding strength [25]. The interfacial structures characters between the reinforcing phases and the Al matrix are consistent with the assumptions of the Kerner model. This is that the Kerner model can predict the CTE of Al6092/SiC/LAS accurately.

It should be noted that the effect of residual thermal stress is not evaluated on the CTE in the Kerner model. When the samples are cooled from high temperature to RT in manufacturing, residual thermal stress develops in MMCs due to the CTE mismatch between reinforcements and matrix [26-28]. Fig. 5a shows the change in elongation of the 5 wt% LAS/35 wt% SiC composite. After three consecutive cycles of testing, the hysteresis region between the curves of the samples is reduced. This hysteresis phenomenon has been reported to be caused by

values predicted by Turner's model [23,24]. It is important to emphasize that the bounds provided by the Kerner model are also influenced by the above mentioned reasons. However, the Kerner model weakens the dominance of the bulk modulus in the model. Especially for the modified model, it is influenced by the combined effect of the normalized CTE and the bulk modulus. This means that the normalized bulk modulus of the reinforcing phases is higher than that of the Al matrix when the content of silicon carbide is higher, which weakens the negative
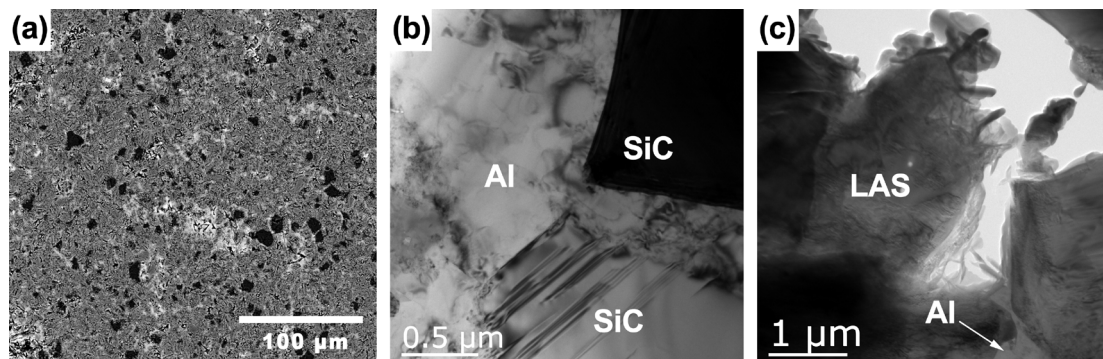

Fig. 4. (a) SEM morphology of Al6092/30wt% SiC/10wt% LAS composites, (b) The interfacial characteristics between Al and SiC, and (c) The interfacial characteristics between Al and LAS
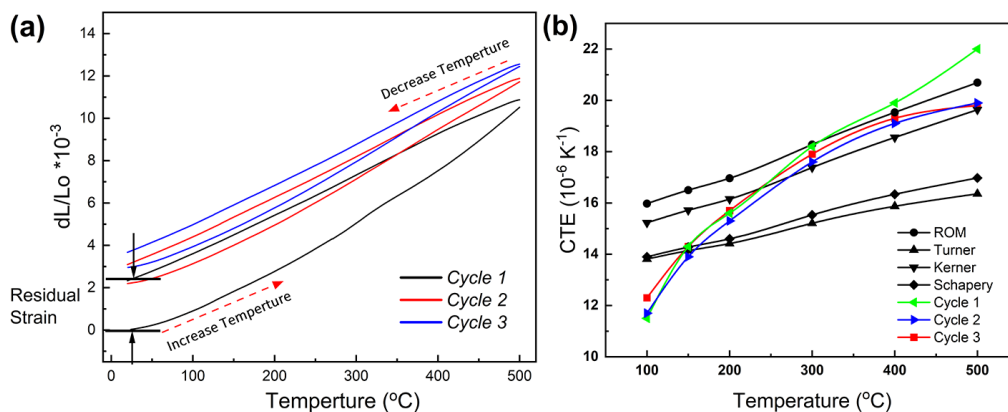

Fig. 5. CTE cycling experiments with the 35 wt% SiC/5 wt% LAS composite: (a) elongation change rate and (b) comparison between predicted and experimental CTE values

1332

thermal stress relaxation in the matrix leading to plastic yield-ing, which is manifested by the cooling shrinkage process not retracing its initial expansion path [29]. As seen in Fig. 5b, the experimental values of the sample without thermal cycle show an upward deviation from the predicted values of the Kerner model. The CTE of this sample requires at least one thermal cycle before it matches the predicted values of the Kerner model. This also confirms that compared to the other models, the Kerner model still does not fully consider the effect of thermal residual stresses generated within the composite during the preparation process on the CTE, despite the fact that it takes more factors and conditions into account and is more realistic. Therefore, the prediction CTE of the Kerner model is often "conservative" compared with the experimental CTE of the sample without thermal cycled. In fact, the ROM, Turner and Schapery models also appear the deviation mentioned above. It is necessary to eliminate the increase in internal stress caused by the structure and processing to obtain a stable CTE value, particularly for multi-phase reinforced MMCs.

4. Conclusion

(1) This paper introduces a new supplementary formulation for the Kerner and Schapery models, which enable them to be applicable to the CTE prediction of multi-phase particle-reinforced composites. Specifically, the CTE, shear modulus, and bulk modulus of multiple reinforcing phases are normalized to a new "single" property by their respective volume fractions.

(2) The thermal expansion properties and morphological characteristics of Al6092/SiC/LAS composites were systematically investigated. A comparison of experimental and predicted CTEs, combining with morphological characterization, indicated the robustness of the modified Kerner model for predicting CTEs of composites with multi-phase near-spherical inclusions.

(3) Although the Kerner model predicts CTE with higher accuracy compared to other thermoelasticity models. However, the Kerner model does not consider the effect of internal stress on CTE. The prediction CTE of the Kerner model is often "conservative" compared with the experimental CTE of the sample without thermal cycled.

REFERENCES

[1] M. Orrhede, R. Tolani, K. Salama, Res. Nondestr. Eval. **8**, 23-37 (1996).

[2] R. Zare, H. Sharifi, M.R. Saeri, M. Tayebi, J. Alloys Compd. **801**, 520-528 (2019).

[3] M. Esmati, H. Sharifi, M. Raesi, A. Atrian, A. Rajaee, J. Alloys Compd. **773**, 503-510 (2019).

[4] M. Tayebi, M. Jozdani, M. Mirhadi, J. Alloys Compd. **809**, 151753 (2019).

[5] C. Hsieh, W. Tuan, Mater. Sci. Eng. A **460**, 453-458 (2007).

[6] P.S. Turner, J. Res. Natl. Bureau Stand. **37**, 237-250 (1946).

[7] E. Kerner, Proc. Phys. Soc. Sect. B **69**, 808 (1956).

[8] R.A. Schapery, J. Compos. Mater. **2**, 380-404 (1968).

[9] S. Elomari, M. Skibo, A. Sundarrajan, H. Richards, Compos. Sci. Technol. **58**, 369-376 (1998).

[10] S. Lemieux, S. Elomari, J. Nemes, M. Skibo, J. Mater. Sci. **33**, 4381-4387 (1998).

[11] Q. Zhang, G. Wu, G. Chen, L. Jiang, B. Luan, Composites Part A **34**, 1023-1027 (2003).

[12] G. Bai, Y. Zhang, J. Dai, L. Wang, X. Wang, J. Wang, M.J. Kim, X. Chen, H. Zhang, J. Alloys Compd. **794**, 473-481 (2019).

[13] L. Yu, S. Jiang, F. Cao, H. Shen, L. Zhang, X. Gu, H. Song, J. Sun, Mater. **14**, 4100 (2021).

[14] N.K. Sharma, R. Misra, S. Sharma, Int. J. Solids Struct. **102**, 77-88 (2016).

[15] R.L. Poveda, S. Achar, N. Gupta, Jom **64**, 1148-1157 (2012).

[16] M. Tayebi, M. Tayebi, M. Rajaee, V. Ghafarnia, A.M. Rizi, J. Alloys Compd. **853**, 156794 (2021).

[17] L. Wang, Z. Xue, Y. Cui, K. Wang, Y. Qiao, W. Fei, Compos. Sci. Technol. **72**, 1613-1617 (2012).

[18] C. Fan, Z. Hu, X. Chen, X. Zhou, L. Ou, J. Yang, Trans. Nonferrous Met. Soc. China **30**, 40-47 (2020).

[19] Y. Jia, F. Cao, S. Scudino, P. Ma, H. Li, L. Yu, J. Eckert, J. Sun, Mater. Des. **57**, 585-591 (2014).

[20] Z. Wei, P. Ma, H. Wang, C. Zou, S. Scudino, K. Song, K.G. Prashanth, W. Jiang, J. Eckert, Mater. Des. **65**, 387-394 (2015).

[21] Z. Hashin, S. Shtrikman, J. Mech. Phys. Solids **11**, 127-140 (1963).

[22] R. Arpon, J. Molina, R. Saravanan, C. Garcia-Cordovilla, E. Louis, J. Narciso, Acta Mater. **51**, 3145-3156 (2003).

[23] M. Vetterli, R. Tavangar, L. Weber, A. Kelly, Scr. Mater. **64**, 153-156 (2011).

[24] H. Holzer, D.C. Dunand, J. Mater. Sci. **14**, 780-789 (1999).

[25] S. Zhang, Q. Hou, H. Jiang, J. Mater. Sci. **57**, 1796-1809 (2022).

[26] O. Matvienko, T. Daneyko, A. Kovalevskaya, I. Khrustalyov, A. Zhukov, Vorozhtsov, Metals **11**, 279 (2021).

[27] Z. Sun, Z. Tian, L. Weng, Y. Liu, J. Zhang, T. Fan, J. Appl. Phys. **127**, 045101 (2020).

[28] X. Wang, J. Yang, P. Chi, E. Bahonar, M. Tayebi, J. Alloys Compd. **901**, 163422 (2022).

[29] M.M. Benal, H. Shivanand, Mater. Sci. Eng. A **435**, 745-749 (2006).